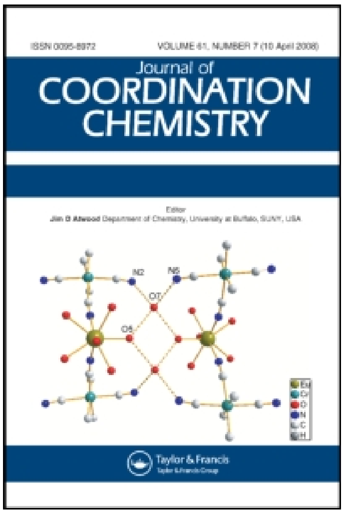

Journal of Coordination Chemistry
Publication details, including instructions for authors and subscription information:
http://www.informaworld.com/smpp/title~content=t713455674

Two binuclear metallamacrocyclic zinc(II) coordination complexes derived from ferrocenecarboxylate and subsidiary ligands: synthesis, crystal structures and properties

Yaru Liu[a]; Zhenyu Cao[b]; Hongwei Hou[a]; Yaoting Fan[a]
[a] Department of Chemistry, Zhengzhou University, Zhengzhou, Henan 450052, P.R. China [b] Textile Institute of Donghua University, Shanghai 200051, P.R. China

To cite this Article Liu, Yaru , Cao, Zhenyu , Hou, Hongwei and Fan, Yaoting(2009) 'Two binuclear metallamacrocyclic zinc(II) coordination complexes derived from ferrocenecarboxylate and subsidiary ligands: synthesis, crystal structures and properties', Journal of Coordination Chemistry, 62: 2, 277 — 286
To link to this Article: DOI: 10.1080/00958970802226379
URL: http://dx.doi.org/10.1080/00958970802226379

Journal of Coordination Chemistry
Vol. 62, No. 2, 20 January 2009, 277–286

Two binuclear metallamacrocyclic zinc(II) coordination complexes derived from ferrocenecarboxylate and subsidiary ligands: synthesis, crystal structures and properties

YARU LIU†, ZHENYU CAO‡, HONGWEI HOU*† and YAOTING FAN†

†Department of Chemistry, Zhengzhou University, Zhengzhou, Henan, 450052, P.R. China
‡Textile Institute of Donghua University, Shanghai 200051, P.R. China

(*Received 26 December 2007; in final form 28 March 2008*)

Two binuclear zinc(II) coordination complexes, $[Zn(FcCO_2)_2(prbbm)]_2 \cdot 2CH_3OH \cdot 2H_2O$ (**1**) (prbbm = 1,1′-(1,3-propanediyl)*bis*-1H-benzimidazole) and $[Zn(FcCO_2)_2(pebbm)]_2 \cdot 4CH_3OH$ (**2**) (pebbm = 1,1′-(1,5-pentanediyl)*bis*-1H-benzimidazole), were obtained by reaction of $Zn(OAc)_2 \cdot 2H_2O$ with sodium ferrocenecarboxylate (FcCOONa) and subsidiary ligands (prbbm or pebbm) in methanol. **1** and **2** are 0-D discrete macrocyclic frameworks with the ferrocenecarboxylate anions as monodentate ligands coordinating to Zn. Their electrochemical and luminescence properties were also investigated.

Keywords: Sodium ferrocenecarboxylate; Subsidiary ligands; Binuclear metallamacrocyclic complexes; Electrochemical and luminescence properties

1. Introduction

The design and preparation of coordination complexes have received much attention because of their structures [1] and widespread potential applications [2–6]. Introducing functional groups to molecular systems has become an important approach to construct coordination complexes with desired properties [7]. As multifunctional ligands, ferrocene carboxylates play an important role in the field because: (1) the versatile coordination modes and strong coordination capacity of the carboxylate group in these ligands make self-assembly of crystal engineering available [8]; (2) ferrocene groups show unusual properties and many ferrocene derivatives have been used as homogeneous catalysts for various processes, molecular sensors, and nonlinear optical (NLO) materials, etc. [9]; (3) the incorporation of ferrocene units into coordination complexes combines the advantages of organometallic complexes with polymer properties and provide an effective method of preparing new functional materials with unique features. Many coordination complexes have been constructed by utilizing ferrocene carboxylate-containing compounds as building blocks. These coordination

---

*Corresponding author. Email: houhongw@zzu.edu.cn

Journal of Coordination Chemistry
ISSN 0095-8972 print/ISSN 1029-0389 online
DOI: 10.1080/00958970802226379

complexes have versatile structures and potential applications in electrochemical sensors, molecular magnetic and nonlinear optical (NLO) materials, etc. [10–14].

In this article, we used the classic ferrocene carboxylate-containing complex, ferrocenecarboxylate ($FcCO_2Na$), as the main ligand to react with Zn(II) in the presence of different bridging ligands and obtained two binuclear metallamacrocycles: $[Zn(FcCO_2)_2(prbbm)]_2 \cdot 2CH_3OH \cdot 2H_2O$ (**1**) (prbbm = 1,1′-(1,3-propanediyl)*bis*-1H-benzimidazole) and $[Zn(FcCO_2)_2(pebbm)]_2 \cdot 4CH_3OH$ (**2**) (pebbm = 1,1′-(1,5-pentanediyl)*bis*-1H-benzimidazole). Herein, we report the syntheses, structural characterizations, electrochemical and luminescence properties of **1** and **2.**

2. Experimental

2.1. *General information and materials*

All chemicals were reagent grade and obtained from commercial sources and used without further purification. $FcCO_2Na$ was prepared according to the literature method [15]. 1,1′-(1,3-propanediyl)*bis*-1H-benzimidazole (prbbm) and 1,1′-(1,5-pentanediyl)*bis*-1H-benzimidazole (pebbm) were prepared according to the literature [16]. Elemental analyses (C, H, and N) were carried out on a Carlo-Erba1106 elemental analyzer. Infrared spectra were recorded on a Bruker TENSOR 27 spectrophotometer with KBr pellets in the 400–4000 cm^{-1} region. ^1H NMR spectra were measured with a BRUKER AM–300 spectrometer in DMF. TGA measurements were performed by heating the sample from 30 to 800°C at a rate of 10°C min^{-1} in air on a NETZSCH STA409PC differential thermal analyzer.

2.2. *Synthesis of $[Zn(FcCO_2)_2(prbbm)]_2 \cdot 2CH_3OH \cdot 2H_2O$ (1)*

A 3 mL methanol-water mixed solution of $FcCO_2Na$ (50.2 mg, 0.2 mmol) was added into a 2 mL methanol solution of $Zn(OAc)_2 \cdot 2H_2O$ (21.9 mg, 0.1 mmol), then 2 mL methanol solution of prbbm (27.6 mg, 0.1 mmol) was added dropwise. The resultant orange solution with pH = 5 ~ 6 was allowed to stand at room temperature in the dark. Red crystals suitable for X-ray diffraction were obtained after ten days. Crystals of **1** are stable in air. Yield: 62% (105.3 mg). IR (cm^{-1}, KBr): 3431s, 3100w, 2933w, 1586s, 1466s, 1387s, 1338m, 746m, 511m. $C_{80}H_{80}Fe_4N_8O_{12}Zn_2$ (1699.70): Calcd C 56.48, H 4.71, N 6.59; found: C 56.53, H 4.64, N 6.56%. ^1H NMR δ(ppm) 2.40 (m, 4H, CH_2), 4.15 (s, 20H, Cp-ring), 4.26 (s, 8H, C_5H_4), 4.42 (m, 8H, NCH_2N), 4.61 (s, 8H, C_5H_4), 7.30 (m, 8H, Ar), 7.66 (m, 4H, Ar), 7.88 (m, 4H, Ar), 8.52 (s, 4H, triazolyl group CH).

2.3. *Synthesis of $[Zn(FcCO_2)_2(pebbm)]_2 \cdot 4CH_3OH$ (2)*

A 3 mL methanol-water mixed solution of $FcCO_2Na$ (50.2 mg, 0.2 mmol) was added into a 2 mL methanol solution of $Zn(OAc)_2 \cdot 2H_2O$ (21.9 mg, 0.1 mmol), then 2 mL methanol solution of pebbm (30.4 mg, 0.1 mmol) was added dropwise. The resulting orange solution with pH = 5 ~ 6 was allowed to stand at room temperature in the dark. Red crystals suitable for X-ray diffraction were obtained after two days. Crystals of **2**

Table 1. Crystal data and structure refinement for **1** and **2**.

Complexes	**1**	**2**
Formula	$C_{80}H_{80}Fe_4N_8O_{12}Zn_2$	$C_{86}H_{92}Fe_4N_8O_{12}Zn_2$
FW	1699.66	1783.82
Crystal system	Monoclinic	Monoclinic
Space group	*P*2(1)/*c*	*P*2(1)/*n*
Unit cells and dimensions (Å, °)		
a	11.830(3)	11.606(2)
b	18.423(4)	21.166(4)
c	19.332(4)	17.055(3)
α	90	90
β	107.464(3)	91.66(3)
γ	90	90
V (Å^3)	4019.0(15)	4188.0(14)
Z	2	2
D_{Calcd} (g cm^{-3})	1.404	1.415
R_1 ($I>2\sigma$)	0.0711	0.0789
wR_2 (all data)	0.2213	0.1943
Goodness of fit	1.008	1.002

are stable in air. Yield: 58% (103.4 mg). IR (cm^{-1}, KBr): 3414m, 3100m, 2937m, 1585s, 1467s, 1387s, 1297m, 748m, 512m. $C_{86}H_{92}Fe_4N_8O_{12}Zn_2$ (1783.86): Calcd C 57.85, H 5.16, N 6.28; found: C 57.89, H 5.11, N 6.32%. ^{1}H NMR δ(ppm) 1.28 (m, 4H, CH_2), 1.825 (m, 8H, CH_2), 4.13 (s, 20H, Cp-ring), 4.25 (s, 8H, C_5H_4), 4.30 (m, 8H, NCH_2N), 4.64 (s, 8H, C_5H_4), 7.30 (m, 8H, Ar), 7.66 (m, 4H, Ar), 7.93 (m, 4H, Ar), 8.60 (s, 4H, triazolyl group CH).

2.4. *Crystal structure determination*

A crystal suitable for X-ray determination is mounted on a glass fiber. The data of **1** were collected at room temperature on a Bruker Aper CCD diffractometer with graphite monochromated Mo-Kα radiation ($\lambda = 0.71073$ Å). The data of **2** were collected at room temperature on a Rigaku Saturn 724 CCD diffractometer with graphite monochromated Mo-Kα radiation ($\lambda = 0.71073$ Å). The structures were solved by direct methods and expanded with Fourier techniques. The non-hydrogen atoms were refined anisotropically. Hydrogen atoms were included but not refined. The final cycle of full-matrix least-squares refinement was based on observed reflections and variable parameters. All calculations was performed with the SHELXL-97 crystallographic software package [17]. Table 1 shows crystal data and processing parameters for **1** and **2**, and table 2 lists selected bond lengths and angles.

2.5. *Electrochemistry*

Electrochemical experiments were performed in a low-volume three-electrode cell in dry, degassed DMF, analyte concentration of 5×10^{-4} M. The background electrolyte was NBu_4ClO_4 (0.1 M). The working electrode was a Pt disk of 2-mm diameter, and the auxiliary electrode was Pt foil. Potentials were reported relative to a commercially available saturated calomel electrolyte. To prevent fouling, the working electrode was polished before each operation. Pure N_2 gas was bubbled through the electrolytic solution to remove oxygen.

Table 2. Selected bond lengths (Å) and angles (°) for **1** and **2**.

1[a]					
Zn(1)–O(2)	1.971(5)	Zn(1)–O(3)	1.949(6)	N(1)–Zn(1)#1	2.004(5)
Zn(1)–N(4)	2.031(5)	Zn(1)–N(1)#1	2.004(5)	O(3)–Zn(1)–N(1)#1	123.8(2)
O(2)–Zn(1)–N(1)#1	111.3(2)	O(3)–Zn(1)–N(4)	103.2(2)	O(2)–Zn(1)–N(4)	98.1(2)
N(1A)–Zn(1)–N(4)	105.9(2)	O(3)–Zn(1)–O(2)	110.8(2)		
2[b]					
Zn(1)–O(1)	1.976(4)	Zn(1)–O(3)	1.941(4)	Zn(1)–N(1)	1.998(4)
Zn(1)–N(4)#1	2.042(5)	N(4)–Zn(1)#1	2.042(5)	O(3)–Zn(1)–N(1)	126.3(2)
O(1)–Zn(1)–N(1)	111.24(19)	O(3)–Zn(1)–N(4)#1	105.2(2)	O(1)–Zn(1)–N(4)#1	98.83(19)
N(1)–Zn(1)–N(4)#1	103.42(18)	O(3)–Zn(1)–O(1)	107.98(19)		

[a] Symmetry transformations used to generate equivalent atoms in **1**: #1 $-x$, $-y+1$, $-z+1$.

[b] Symmetry transformations used to generate equivalent atoms in **2**: #1 $-x+1$, $-y$, $-z+1$.

2.6. *Determination of fluorescent properties*

The luminescent spectra were measured on powder samples at room temperature using an F-4500 HITACHI fluorescence spectrophotometer. The excitation slit and the emission slit were 5 nm; the response time was 2 s.

3. Results and discussion

3.1. *Crystal Structure of $[Zn(FcCO_2)_2(prbbm)]_2 \cdot 2CH_3OH \cdot 2H_2O$ (1)*

X-ray diffraction analysis reveals that **1** is a neutral binuclear metallamacrocycle with a crystallographic center of symmetry [figure 1(a)]. The binuclear metallamacrocycle is composed of two Zn(II) ions, two bridging prbbm ligands, and four monodentate ferrocenecarboxylate anions.

Each Zn(II) is in a slightly distorted tetrahedral environment with two oxygens (O2 and O3) from two ferrocenecarboxylates and two nitrogens (N1A and N4) from two prbbm. The Zn–O lengths are 1.971(5) and 1.949(6) Å, while the Zn–N lengths are 2.004(5) and 2.031(5) Å. The Zn–N distances are slightly shorter than those of reported Zn(II) coordination complexes, indicating strong interaction between Zn and N. Examples are $[Zn(4,4'\text{-bipy})(H_2O)_3(ClO_4)](ClO_4) \cdot (4,4'\text{-bipy}) \cdot 1.5H_2O$ (Zn–N: 2.104(2)–2.117(2) Å) [18a], [Zn(tp)(4,4′-bipy)] (tp = terephthalate) (Zn–N: 2.154(2)–2.186(3) Å) [18b] and $[Zn(fca)_2(bpe)]_n \cdot 2nH_2O$ (fca = $C_5H_5FeC_5H_4C(OH)CHCOCH_3$) (Zn–N: 2.196(8)–2.205(8) Å) [18c]. The bond angles around each Zn(II) range from 103.2(2) to 123.8(2)°, except for the acute O(2)–Zn(1)–N(4) angle of 98.1(2)°. Hence, the average bond angle at Zn1 is 108.8(7)°, slightly smaller than 109.5° for an ideal tetrahedron.

The zinc-zinc distance is 9.333 Å in each metallamacrocycle. Between adjacent $[Zn(FcCO_2)_2(prbbm)]_2$ units, the benzimidazole rings are parallel with average interplanar distance of 3.48 Å, which is in the range for π–π interactions between two aryl rings [19]. These π–π interactions among benzimidazole rings and hydrogen bonds between $[Zn(FcCO_2)_2(prbbm)]_2$ and solvent molecules link the discrete binuclear macrocyclic units into a 1-D infinite chain, as shown in figure 1(b). Although the π–π interactions are weak, they are important in the molecular assembly.

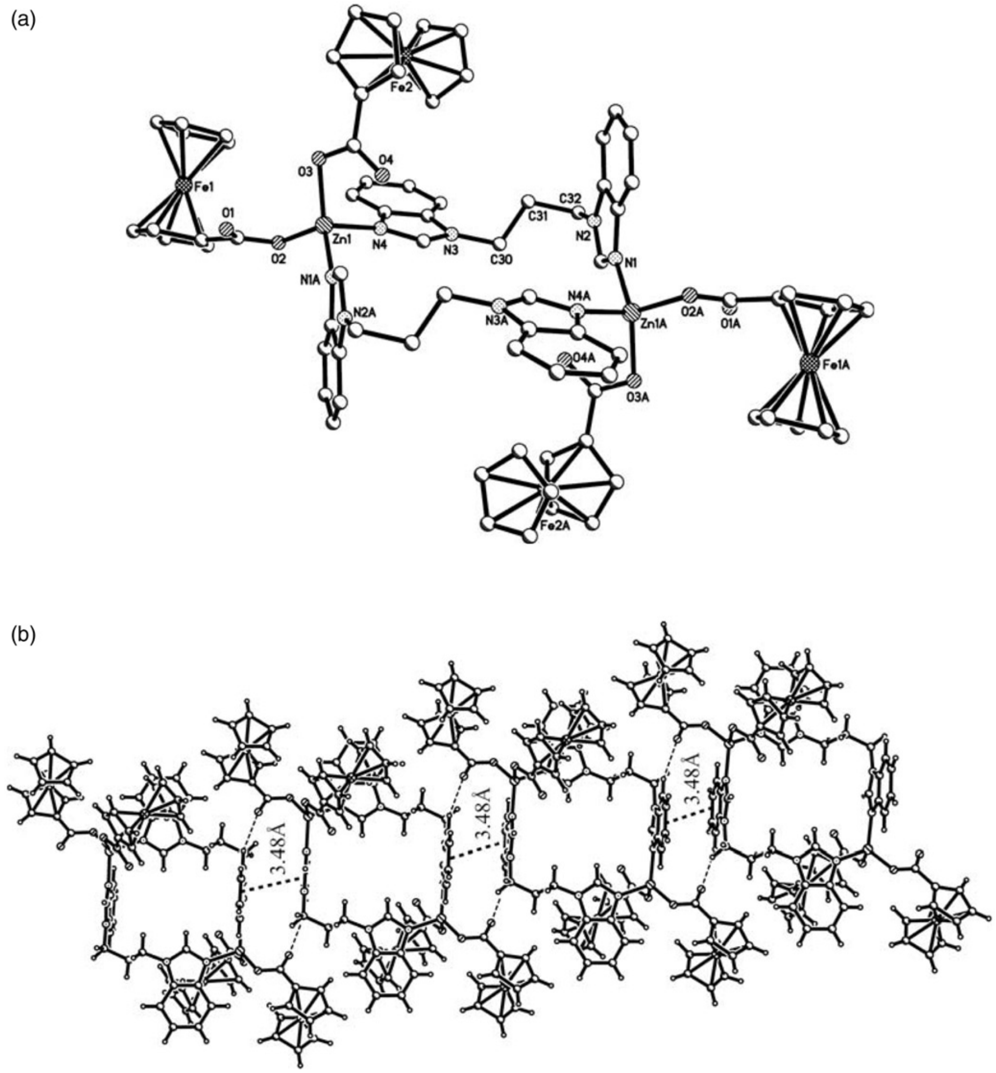

Figure 1. (a) Perspective view of **1** showing the atom numbering scheme. All hydrogen atoms and solvent molecules are omitted for clarity. (b) View of 1-D chain in **1** showing the π–π interactions and hydrogen bonds.

3.2. *Crystal structure of $[Zn(FcCO_2)_2(pebbm)]_2 \cdot 4CH_3OH$ (2)*

Complex **2** [figure 2(a)] has a similar structure to **1**. The binuclear metallamacrocycle is composed of two Zn(II) ions, two bridging pebbm ligands, and four ferrocenecarboxylate anions. The Zn–O lengths are 1.976(4) and 1.941(4) Å, and the Zn–N lengths are 1.998(4) and 2.042(4) Å. The bond angles around each Zn(II) ion range from 103.3(9) to 126.3(3)°, aside from the acute O(2)–Zn(1)–N(4) angle of 98.8(8)°. Average bond angle at Zn1 is 108.8(3)°, similar to those of **1**. In each metallamacrocycle, the distance between the two zinc atoms is 11.859 Å, which is longer than that of **1** due to the different lengths of the pebbm and prbbm ligands. Benzimidazole rings between adjacent $[Zn(FcCO_2)_2(pebbm)]_2$ units are parallel with the average interplanar distance of 3.4817 Å, similar to that of **1**. Like **1**, these π–π interactions among benzimidazole rings and hydrogen bonds between $[Zn(FcCO_2)_2(pebbm)]_2$ and solvent molecules link the discrete binuclear macrocyclic units into a 1-D infinite chain, as shown in figure 2(b).

In previous work, we have obtained an infinite one-dimensional helical chain $\{[Zn(FcCOO)_2(bbbm)] \cdot 2H_2O\}_n$ (bbbm = 1,1′-(1,4-butanediyl)-*bis*-1H-benzimidazole) by reaction of $Zn(OAc)_2 \cdot 2H_2O$ with bbbm and FcCOONa in methanol [20]. Obviously, the structure of $\{[Zn(FcCOO)_2(bbbm)] \cdot 2H_2O\}_n$ is different to those of **1** and **2** although the three complexes contain similar bridging ligands. The difference can be explained by different conformational flexibility among the pebbm, bbbm and prbbm ligands. A conformationally flexible ligand usually leads to structural diversification of the products. For example, many coordination polymers containing the flexible ligand bpp have multifarious-dimensional structures because the bpp molecule [1,3-*bis*(4-pyridyl)propane] can adopt TT, TG, GG, and GG′ conformations

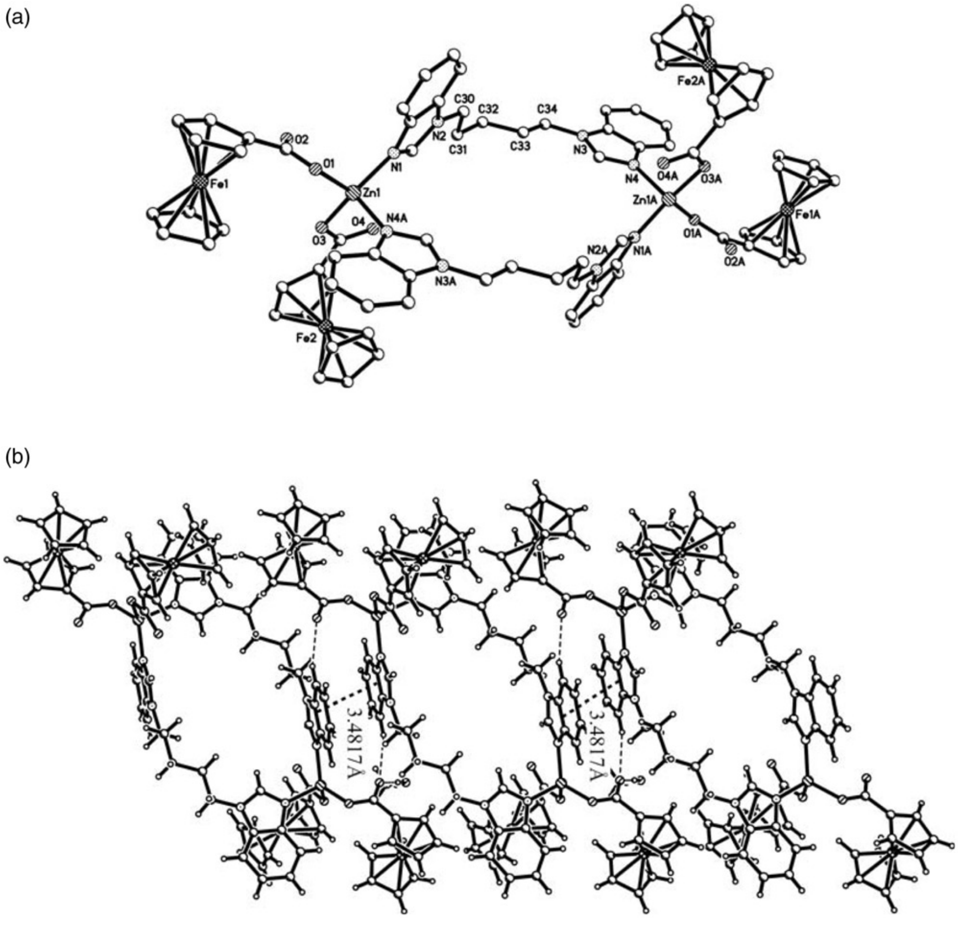

Figure 2. (a) Perspective view of **2** showing the atom numbering scheme. All hydrogen atoms and solvent molecules are omitted for clarity. (b) View of 1-D chain in **2** showing the π–π interactions and hydrogen bonds.

(where T = trans and G = gauche). The prbbm in **1** adopts GT conformation [the torsional angles of the fragments of N2–C32–C31–C30 and C32–C31–C30–N3 are 81.88, 175.56, respectively]; pebbm in **2** adopts TGTT conformation [the torsional angles of the fragments of N2–C30–C31–C32, C30–C31–C32–C33, C31–C32–C33–C34, and C32–C33–C34–N3 are 178.29, 70.15, 172.66 and −175.65, respectively]. As a result, prbbm and pebbm molecules with these conformations are inclined to link two Zn(II) ions simultaneously, inducing formation of the double-bridge and binuclear structure. In $\{[Zn(FcCOO)_2(bbbm)] \cdot 2H_2O\}$, bbbm adopts GTG conformation [the torsional angles of the fragments of N4–C39–C40–C40A, C39–C40–C40A–C39A and C40–C40A–C39A–N4A are 58.70°, 180° and 58.70°, respectively], indicating that the relative orientation of benzimidazole groups of bbbm in $\{[Zn(FcCOO)_2(bbbm)] \cdot 2H_2O\}_n$ is different from that of pebbm or prbbm in **1** or **2**. Such bbbm groups can be propagated in one direction and in this way a 1-D chain arises. The length and especially the conformational flexibility of alkyl spacers, as well as the rotational freedom of the benzimidazole rings observed in the auxiliary ligands, are responsible for the relative orientations of N donors, giving different structures of coordination complexes.

3.3. *Electrochemical properties*

The ^{1}H NMR spectra data of complexes **1** and **2** prove that the structures of complexes **1** and **2** keep unchanged in DMF. The solution-state differential pulse voltammograms of **1**, **2** and NaOOCFc in DMF solution show single peaks with half-wave potentials at 0.712 V for **1**, 0.704 V for **2**, and 0.423 V for NaOOCFc (*vs.* SCE) (figure 3). Obviously, the half-wave potential of **1** and **2** shifted to higher potentials compared with that of the free NaOOCFc. The central metal in these complexes has influence on the half-wave potential of the ferrocenyl moieties, shifting the Fe^{II}/Fe^{III} oxidation potential of ferrocene-containing complexes to higher potential, consistent with our

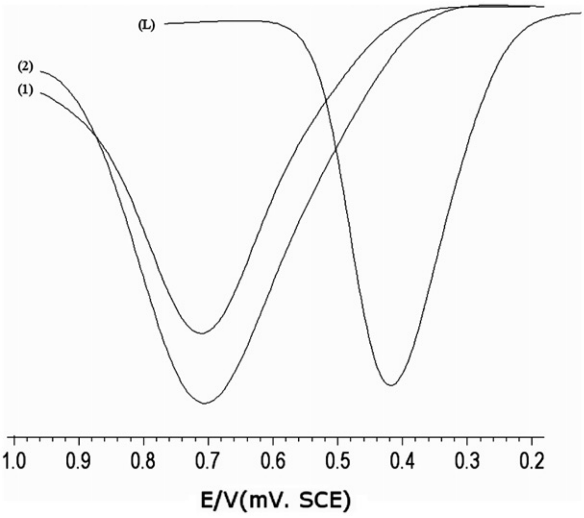

Figure 3. Differential pulse voltammograms of **1**, **2** and the corresponding ferrocenyl ligand, FcCOONa (**L**) in DMF containing $[Bu_4N][ClO_4]$ (0.1 M) at a scan rate of $20\,mV\,s^{-1}$.

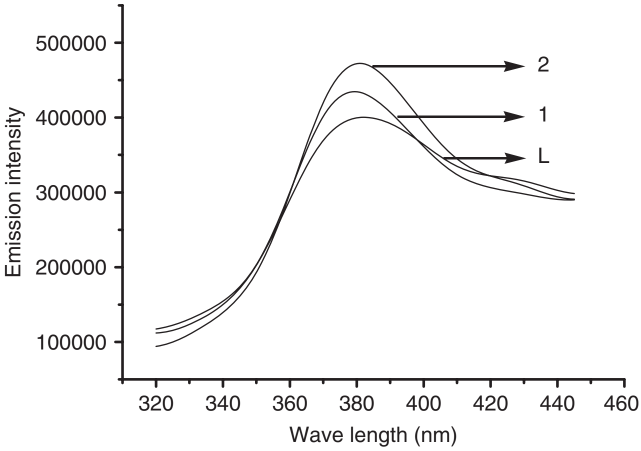

Figure 4. Emission spectra of **1**, **2** and sodium ferrocenecarboxylate (**L**) in solid state at room temperature.

previous results [21]. The electron-withdrawing nature of the coordinated metal center makes the ferrocene unit harder to oxidize.

3.4. *Fluorescence properties*

The fluorescence properties of **1**, **2** and sodium ferrocenecarboxylate are measured in the solid state at room temperature (figure 4). The exciting wavelengths are 245 nm, the maximum emission peaks are at 390 nm for **1**, 391 nm for **2**, and 391 nm for NaOOCFc. Obviously, the fluorescence peak positions of **1**, **2** and NaOOCFc are very close, implying that the fluorescence emissions of **1** and **2** are by NaOOCFc. Therefore, we suggest that the fluorescence emissions observed in **1** and **2** can be assigned to the ligand-to-ligand charge transfer (LLCT) emissions. In our previous article, similar photoluminescences were reported for 1,1′-ferrocenedicarboxylate complexes, binuclear $[M_2(\eta^2\text{-}O_2CFcCO_2)_2(2,2'\text{-bpy})_2(H_2O)_2]$ (M = Cd; Zn) and $[M_2(O_2CFcCO_2)_2(2,2'\text{-bpy})_2(\mu_2\text{-}OH_2)_2]$ (M = Co; Ni) [19a], 1-D wave-shaped polymer $\{[Cd(\eta^2\text{-}O_2CFcCO_2\text{-}\eta^2)(H_2O)_3]\cdot 4H_2O\}_n$ and the 2-D layered polymers $\{[M(\eta^2\text{-}O_2CFcCO_2\text{-}\eta^2)(\mu_2\text{-}\eta^2\text{-}O_2CFcCO_2\text{-}\eta^2\text{-}\mu_2)_{0.5}(H_2O)_2]\cdot mH_2O\}_n$ (M=Tb^{3+}, Eu^{3+}, Y^{3+}; $m = 1$ or 2) [22]. All have maximum emissions in the range 390 nm to 393 nm, showing that the fluorescence mechanism of ferrocenyl is independent of the structure.

3.5. *Thermogravimetric analysis (TGA)*

1 loses weight from 30 to 114°C corresponding to loss of H_2O and CH_3OH. Multiple weight loss steps in the temperature range 250–480°C correspond to decomposition of $FcCOO^-$ and prbbm. A brown amorphous residue of ZnO + 2FeO remained. Finally, a plateau region is observed from 480 to 800°C. There are two very strong exothermic peaks at 272 and 425°C on the DTA curve. **2** first loses solvent from 30 to 121°C and secondly goes through complicated multiple weight loss steps in the temperature range 254–475°C corresponding to the decomposition of $FcCOO^-$ and pebbm. A brown amorphous residue of ZnO+2FeO remained. There is a very strong exothermic peak at 441°C on the DTA curve. The thermal results are in reasonable agreement with the crystal structure analyses of **1** and **2**.

Supplementary material

CCDC 671811 and 671812 for **1** and **2** contain the supplementary crystallographic data for this article. These data can be obtained free of charge via http://www.ccdc.cam.ac.uk/conts/retrieving.html, or from the Cambridge Crystallographic Data Centre, 12 Union Road, Cambridge CB2 1EZ, UK [Fax: (+44) 1223-336-033; or E-mail: deposit@ccdc.cam.ac.uk].

Acknowledgement

This work was supported by the National Natural Science Foundation of China (Nos. 20671082 and 20371042) and NCET.

References

[1] S.W. Keller. *Angew. Chem. Int. Ed. Engl.*, **36**, 247 (1997).

[2] P.J. Hagrman, D. Hagrman, J. Zubieta. *Angew. Chem. Int. Ed. Engl.*, **38**, 2638 (1999).

[3] X.R. Meng, Y.L. Song, H.W. Hou, Y.T. Fan, G. Li, Y. Zhu. *Inorg. Chem.*, **42**, 1306 (2003).

[4] F. Lloret, G.D. Munno, M. Julve, J. Cane, R. Ruiz, A. Caneschi. *Angew. Chem. Int. Ed. Engl.*, **37**, 135 (1998).

[5] C.L. Bowes, G.A. Ogin. *Adv. Mater.*, **8**, 13 (1996).

[6] M. Kondo, T. Yoshitomi, K. Seik, H. Matsuzaka, S. Kitagawa. *Angew. Chem. Int. Ed. Engl.*, **36**, 1725 (1997).

[7] (a) E.K. Efthimiadou, N. Katsaros, A. Karaliota, G. Psomas. *Inorg. Chim. Acta*, **360**, 4093 (2007); (b) W.A. Volkert, T.J. Hoffman. *Chem. Rev.*, **99**, 2269 (1999).

[8] (a) R. Cao, D. Sun, U. Liang, M. Hong, K. Tatsumi, Q. Shi. *Inorg. Chem.*, **41**, 2087 (2002); (b) O.M. Yaghi, C.E. Davis, G.M. Li, H.L. Li. *J. Am. Chem. Soc.*, **119**, 2861 (1997).

[9] (a) P. Beer, D.K. Smith. *Pron. Inorg. Chem.*, **46**, 1 (1997); (b) J.S. Miller, A.J. Epstein. *Angew. Int. Ed. Engl.*, **33**, 385 (1994); (c) P. Nguyen, P. Gomea-Elipe, I. Manners. *Chem. Rev.*, **99**, 1515 (1999); (d) N.G. Long. *Angew. Chem. Int. Ed. Engl.*, **34**, 21 (1995).

[10] D. Guo, B.G. Zhang, C.Y. Duan, X. Cao, Q.J. Meng. *J. Chem. Soc., Dalton Trans.*, 282 (2003).

[11] G.L. Zheng, J.F. Ma, Z.M. Su, L.K. Yan, J. Yang, Y.Y. Li, J.F. Liu. *Angew. Chem. Int. Ed.*, **43**, 2409 (2004).

[12] G. Li, H.W. Hou, L.K. Li, X.R. Meng, Y.T. Fan, Y. Zhu. *Inorg. Chem.*, **42**, 4995 (2003).

[13] V. Chandrasekhar, S. Nagendran, S. Bansal, M.A. Kozee, D.R. Powell. *Angew. Chem. Int. Ed.*, **39**, 1833 (2000).

[14] K.C. Kumara Swamy, S. Nagabrahmanandachari, K. Raghuraman. *J. Organomet. Chem.*, **587**, 132 (1999).

[15] *Gmelin Handbuch der Anorganische Chemie*, *Eisen Organische Verbindungen*, Springer-Verlag, Berlin, Vol. A3, p. 58 (1976).

[16] X.J. Xie, G.S. Yang, L. Cheng, F. Wang. *Huaxue Shiji*, **22**, 222 (2000).

[17] G.M. Sheldrick. *SHELXL-97*, *Program for Refinement of Crystal Structure*, University of Göttingen, Germany (1997).

[18] (a) M.L. Tong, J.W. Cai, X.L. Yu, X.M. Chen, S.W. Ng, T.C.W. Mak. *Aust. J. Chem.*, **51**, 637 (1998); (b) J. Tao, M.L. Tong, X.M. Chen. *J. Chem. Soc.*, *Dalton Trans.*, 3669 (2000); (c) G. Li, H.W. Hou, Y. Zhu, X.R. Meng, L.W. Mi, Y.T. Fan. *Inorg. Chem. Commun.*, **5**, 929 (2002).

[19] (a) S.L. Zheng, J.H. Yang, X.L. Yu, X.M. Chen, W.T. Wong. *Inorg. Chem.*, **43**, 830 (2004); (b) X.L. Zhang, X.M. Chen. *Cryst. Growth Des.*, **5**, 617 (2005).
[20] G. Li, Z.F. Li, H.W. Hou, X.R. Meng, Y.T. Fan, W.H. Chen. *J. Mol. Struct.*, **694**, 179 (2004).
[21] (a) H.W. Hou, G. Li, L.K. Li, Y. Zhu, Y.T. Fan. *Inorg. Chem.*, **42**, 428 (2003); (b) H.W. Hou, L.K. Li, G. Li, Y.T. Fan, Y. Zhu. *Inorg. Chem.*, **42**, 3501 (2003).
[22] X.R. Meng, G. Li, H.W. Hou, H.Y. Han, Y.T. Fan, Y. Zhu, C.X. Du. *J. Organomet. Chem.*, **679**, 153 (2003).